Wood Science and Technology
https://doi.org/10.1007/s00226-020-01212-2

ORIGINAL

Anisotropic electrical conductivity of green timber within 20 − 90°C temperature range

N. Nursultanov[1] · W. J. B. Heffernan[1] · C. Altaner[2] · S. Pang[3]

Received: 24 February 2020

Abstract

Electrical conductivity (EC) of the unseasoned timber of three softwood species (*Pinus radiata*, *Pseudotsuga menziesii*, and *Sequoia sempervirens*) and one hardwood species (*Eucalyptus globoidea*) was studied over the temperature range of 20 – 90°C. EC was measured in sapwood, transitional wood, and heartwood in the three principle grain directions. All species exhibited similar behaviour: (1) heartwood EC was lower than that of sapwood and (2) EC increased with temperature. *P. radiata* samples from two regions of New Zealand's South Island showed variation of EC by a factor of two in the longitudinal direction; however, in the radial and tangential directions, the EC variation was less pronounced. This work seeks to provide possible explanations for EC variation in green wood and to propose suggestions for future research.

Introduction

Growing interest in various plant and wood related technologies such as precision irrigation (Oletic and Bilas 2020), earlier plant disease detection (Khaled et al. 2018), electrical heating of wood (Hoover et al. 2010; Heffernan et al. 2018), and sapwood/heartwood identification in living trees (Guyot et al. 2013) require holistic understanding of wood properties. However, some of the wood properties such as electrical conductivity (EC) have been studied partially, with most of the research done on wood below fibre saturation point (FSP), which is commonly assumed to be around 30% MC (Berry and Roderick 2005), and at near room temperature. Such limited interest in EC peaked after Stamm (1927, (1930)

✉ N. Nursultanov
nurzhan.nursultanov@epecentre.ac.nz

[1] EPECentre, University of Canterbury, Private Bag 4800, Christchurch 8140, New Zealand

[2] School of Forestry, University of Canterbury, Private Bag 4800, Christchurch 8140, New Zealand

[3] Chemical and Process Engineering, University of Canterbury, Private Bag 4800, Christchurch 8140, New Zealand

Published online: 10 August 2020

found that wood EC is linearly correlated with moisture content (MC) below FSP, while the overall effect of the full range of MC on EC is nonlinear. This correlation formed the basis for all electrical moisture meters. However, to develop and improve emerging technologies such as Joule heating (Heffernan et al. 2018), a holistic knowledge of EC is desirable, below and above FSP. Only then, such knowledge, coupled with suitable electrodes (Heffernan et al. 2018), would enable accurate determination of sapwood and heartwood proportions of green logs and live trees, temperature/temperature distribution measurement of heated logs and, in conjunction with a computational model, prediction and control of Joule heating of logs for phytosanitary (Nursultanov et al. 2019) or other conditioning purposes. In addition, knowing wood EC above FSP would allow improvement in the accuracy of established technologies such as electrical resistance tomography (ERT), which estimates electrical resistivity (the reciprocal of EC) distribution computationally (Guyot et al. 2013; Luo 2019).

The complex structure of wood has a major effect on its EC. When oven-dried, wood is an insulator, with an EC of $10^{-15} - 10^{-16}$ S m^{-}1 (Glass and Zelinka 2010), while green wood containing water and minerals in the sap, is an electrical conductor (Fleischer and Downs 1953). Below FSP, MC has the most pronounced effect on EC of wood. For example, in the range between 7% and FSP, EC increases up to four times per 1% increase in MC. The total increase in EC from the oven-dry condition to FSP, with EC of $10^{-3} - 10^{-4}$ S m^{-}1, is over 10^{10} times (Glass and Zelinka 2010). Such increase in EC was explained by establishment of overlapping conductive paths at some percolation threshold (Zelinka et al. 2008). According to Zelinka et al. (2015), initially assumed to be at about 16% of MC, this percolation threshold depends on ion types, cell wall layer, and grain orientation, resulting in different threshold values, which are generally below FSP. The conducting ions do not move unless a threshold MC is reached, softening hemicelluloses and resulting in formation of diffusion channels. The hemicellulose softening process starts slightly below the percolation threshold and gradually continues until a network of diffusion channels is established, allowing chemical and ionic conduction and increasing EC (Zelinka et al. 2008). Conduction of electrical current below or near FSP occurs through cell walls, as wood voids are filled with air or vapour, which are non-conductive. Above FSP, conduction of electrical current is unknown, as moisture distribution paths are erratic (Skaar 1988). Thus, without knowing the electrical current conduction mechanism above FSP, using relatively large testing samples is more appropriate due to minimisation of the effect of cellular structure on EC.

Effect of temperature below FSP is nonlinear and less pronounced than that of MC (Skaar 1988). At 10% MC, a temperature rise from 20 to 80 °C increases EC of wood from approximately 10^{-8} to about 10^{-5} S m^{-1} (Skaar 1988). However, above FSP, the effect of temperature on EC becomes dominant (Nursultanov et al. 2017), with the effect of MC being negligible (Stamm 1929, 1964; Nursultanov et al. 2017). The effect of temperature on the longitudinal EC of green *P. radiata* is near linear, similar to aqueous solutions of salts below water's boiling point (McCleskey 2011; Haynes 2014), while in the radial and tangential directions, the effect remains nonlinear (Nursultanov et al. 2017).

Temperature, however, does not have a direct effect on the EC of ionic solutions, which depends on three parameters: ion concentration, charge magnitude, and ionic mobility, with the whole relationship expressed as (Bard and Faulkner 2001):

$$\sigma_{\text{sap}} = F \sum_{i} |z_i| u_i C_i, \tag{1}$$

where σ_{sap} is the sap electrical conductivity, F is the Faraday constant, i is the ionic species, $|z|$ is the charge magnitude, u is the mobility, and C is the ionic concentration. This equation shows that EC of wood would depend on the ion content of soil and its variation around a year; for example some trees may be in a hibernation state during winter, with no sap flowing. In addition, there could be a change in ion concentration caused by droughts and rainy seasons; for example in desiccated soil, ions cannot flow towards roots and hence, there will not be an ionic flow in trees. Finally, ionic distribution within a tree can be non-uniform, resulting in difference of EC between two adjacent samples.

On the other hand, during an electrical conductivity experiment, a tested wood sample does not absorb new ions nor desorb its ions to the surrounding. [Absorption and desorption of ions could occur if the material used for joining electrodes and a sample contains a fluid with mobile ions, such as an electrically conductive gel (Nursultanov et al. 2017)]. There could be some ion losses at the contacts due to oxidation of the electrodes, which is negligible relative to the total number of ions within the sample. Thus, the only parameter which must vary with temperature during wood electrical conductivity measurement is the ionic mobility, which can be described as (Bard and Faulkner 2001):

$$u_i = \frac{|z_i| e}{6\pi\eta r}, \tag{2}$$

where e is the electronic charge, η is the medium viscosity, and r is the ion radius. In this equation, the only non-constant parameter is viscosity, which decreases in fluid with a temperature increase. In the range from 20 to 90°C, the dynamic viscosity of water drops by a factor of three, from 1.003×10^{-3} to 0.316×10^{-3} N s m^{-2} (White 2011). Hence, if the increase in wood EC follows the decrease in water viscosity, it can be hypothesised that electrical current conduction in wood is similar to that in an ionic solution. In other words, conduction of electrical current by means of ions is unconstrained by wood structure.

The wood structure varies in the longitudinal (L), radial (R), and tangential (T) directions, making EC directionally dependent, or anisotropic. Generally, EC in the longitudinal direction is much higher than in the other directions, with the radial EC being slightly higher than the tangential conductivity (Stamm 1929). According to Kuroda and Tsutsumi (1982), the anisotropy of the EC of *Cryptomeria japonica* depends on the MC. The authors found that the ratio of longitudinal to tangential conductivities decreased from about eight, at a MC of 1.5%, to two, at a MC of 8.5%, but then the ratio increased linearly to almost four between 8.5 and 20% MC. Studying eight United States species within a 10–15% MC range, Stamm (1960) found that the ratio of the longitudinal to tangential conductivity varied from 2.1 to

3.9 and the ratio of the longitudinal to radial conductivity ranged from 1.9 to 3.2. However, Stamm (1960) stated that anisotropy of EC is independent of MC. The ratios of longitudinal to radial and tangential conductivities vary with temperature (Nursultanov et al. 2017). In green *P. radiata* at 20°C, the ratios of the longitudinal to radial and the longitudinal to tangential EC were 10 and 20, respectively, while at 90°C these ratios decreased to 7 and 10, respectively. Overall, in the range from 20 – 90°C, the longitudinal, radial, and tangential electrical conductivities of New Zealand grown *P. radiata* increase 3.2, 4.3, and 6.1 times, respectively (Nursultanov et al. 2017). The increase in the longitudinal EC is comparable to the decrease in water viscosity. In the radial and tangential directions, the EC increase is notably greater, indicating that wood structure in the transverse directions has a greater effect on EC. The previous study by Nursultanov et al. (2017), however, is limited to a single provenance of a single species (*P. radiata*) represented by samples from two boards. There appear to be no similar studies, which could verify this observation, in the literature.

The earlier studies of wood EC were done on rectangular blocks (Stamm 1927, 1960) or transverse discs (Stamm 1929) clamped between two plate-type electrodes. Conduction of electrical current in this configuration goes from one flat contact surface to the opposite one. The main benefit of this method is that an electrical current flows through a known surface area along a known length. Thus, EC can be easily calculated from electrical resistance, using Ohm's law from measured current and voltage. If the rectangular blocks are cut along the principle grain directions, EC measurements can be made in the L, R, and T directions (Nursultanov et al. 2017), while transverse discs allow EC measurements solely in the L direction. To measure the spatial electrical resistivity distribution within wood, ERT uses multiple pin-type electrodes attached around a sample. The main benefit of ERT is that it provides a spatial, two-dimensional distribution of electrical resistivity lying on the cross-sectional plane formed by the pin-type electrodes, without tree harvesting. However, ERT estimates only the transverse resistivity distribution, which is a combination of the R and T resistivity values. As ERT back-calculates the resistivity distribution from experimental voltage and current data, the results contain an unavoidable calculation error. Both plate- and pin-type electrodes require firm contact with the sample to avoid high-contact resistance. The pin-type electrodes rely on direct physical contact with the wood, whereas plate-type electrodes must conform to the uneven contact surface of the wood. Therefore, using plate-type electrodes, Stamm (1960) used mercury to improve the contact, while Nursultanov et al. (2017) used silver foam with gold leaf attached to the wood surface. In addition, Nursultanov (2018) applied electrically conductive gel, an aqueous mixture of psyllium husk and sodium chloride, on the wood contact surface to minimise contact resistance; however, he found that sodium chloride penetrates into the wood affecting the measurement.

The main objective of this study is to verify the correlation between wood electrical conductivity and water viscosity by measuring EC in the principle directions (L, T, and R) at various temperatures of three softwood species: *Pseudotsuga menziesii*, *Sequoia sempervirens*, and *P. radiata* and one hardwood species: *Eucalyptus globoidea*. In addition, effects of tree origin and wood dryness on EC were studied, based on *P. radiata* samples. The effect of ionic composition of soil, the distribution of ions within wood, and wood cellular structure on EC are not covered in this research.

Materials and methods

Materials

Five logs, of four New Zealand grown wood species, from three regions of the South island, were selected in this research (Table 1). The logs were approximately 1 m long and stored at −20°C. Each log's heartwood (HW), sapwood (SW), and transitional wood (TW), if existing, zones were identified by visual means. Each log was cut along the length into 1 m long strips with a cross section of 30 × 30 mm. The *E. globoidea* log had a sapwood section only about 20 mm wide and hence its strips were trimmed to a cross section of 20 × 30 mm. Strips containing either pure sapwood, pure heartwood, or pure transitional wood were selected for the experiments. The strips were chopped into 30 mm long blocks. To allow EC measurement in the radial and tangential directions, only flat- and quarter-sawn blocks were selected. Thus, each side of the blocks aligned either with the radial (R), tangential (T), or longitudinal (L) direction. As the size of the TW and HW zones within *S. sempervirens* and the HW zone within *P. menziesii* were relatively small, the blocks from these zones did not have straight grains in the R and T directions. Hence, these blocks were used only for estimating the longitudinal EC. Finally, some earlier experiments on *P. radiata* boards (Nursultanov 2018), showed that EC in the L direction of pure HW boards was about 0.001 $S\,m^{-}1$ at room temperature, nearly forty times lower than the EC of *P. radiata's* SW in the L direction (Nursultanov et al. 2017). Therefore, in this study, only the sapwood EC of *P. radiata* was studied.

Table 1 Origin, age, wood types (WT), basic density (BD), moisture content (MC), and number of samples per direction for each studied specimen

Wood species	Origin	Age	WT[a]	BD	MC	No. Samples[a,b]		
				($Kg\,m^{-3}$)	(%)	L	R	T
P. menziesii	Nelson Owen River forest	17	HW	407 ± 14	48.4 ± 0.9	8	-	-
			SW	449 ± 19	143 ± 12	12	8	8
S. sempervirens	Nelson Owen River forest	13	HW	385 ± 17	183 ± 8	8	-	-
			TW	316 ± 5	145 ± 6	8	-	-
			SW	310 ± 13	256 ± 14	8	8	8
P. radiata	Canterbury Ashley forest	27	SW	465 ± 29	135 ± 15	19	8	8
P. radiata	Nelson Owen River forest	10	SW	355 ± 7	206 ± 6	16	12	12
E. globoidea	Marlborough Tai Tane forest	14	HW	398 ± 14	174 ± 11	12	12	8
			SW	410 ± 9	162 ± 8	24	6	6

[a] HW, TW, and SW denote heartwood, transitional wood, and sapwood zones, respectively.

[b] L, R, and T denote the longitudinal, radial, and tangential directions, respectively

Fig. 1 **a** *P. radiata* log from Owen River forest (Nelson region) with the internally developed dry patches and **b** the blocks of various dryness, showing the four right hand blocks selected for EC measurements on partially dried wood

Table 2 MC and BD of the *P. radiata* blocks from Owen River forest with dry patches

Block No.[a]	MC (%)	BD [Kg m^3]
Block 1	195	358
Block 2	198	342
Block 3	153	358
Block 4	115	364
Block 5	107	363
Block 6	99	365
Block 7	96	359
Block 8	50	363
Block 9	30	364

[a] The blocks used for the EC measurement are shown in bold

The *P. radiata* log from Owen River forest had some dry patches along the length, as shown in Fig. 1a.

Hence, to determine the effect of temperature on EC and compare this log with the other logs, the forty sample sapwood blocks of Table 1 were cut exclusively out of the wet patches. However, nine additional sapwood blocks of various dryness were also cut out of the log (Fig. 1b), to study the effect of water loss on EC, with their MC and basic density (BD) shown in Table 2. To reduce the number of measurements, only four of these blocks (Block 1, 4, 7, and 9) were selected for EC measurement in the L direction.

Electrical conductivity measurement

Prior to the experiment, four randomly chosen blocks were taken out the freezer and left overnight at room temperature inside a zipped plastic bag for thermal equilibration. Then, each block was weighed, to determine green mass, and the length of each side was measured with a calliper. To reduce contact resistance between the electrodes and the blocks, the contact surfaces were covered with gold leaves, produced by Noris Blattgold GmbH (Fig. 2a).

Afterwards, each block was clamped between two brass electrodes and positioned into a plastic enclosure to stop significant moisture loss. The surface of the electrodes was covered with silver foam (SOFT-SHIELD 4850 from Parker Chomerics) to improve the contact area and fill the air gaps between contact surfaces and electrodes. Thereafter, the plastic enclosures with blocks inside were weighed and put into an oven initially kept at room temperature. Using a programmable AC electric power source (Chroma 61504), a sinusoidal voltage of 50 or 33.3 V at 400 Hz was applied across each sample, with only one sample being tested at a time (Fig. 2b). Two voltage levels ensured the same electric field across 30 or 20 mm long blocks. The current flowing through the sample and the voltage drop across the sample were measured by KEYSIGHT U340461A and KEYSIGHT U3402A meters, respectively. To avoid significant Joule heating, the duration of excitation was 3 seconds. After recording the electrical data at room temperature, the temperature in the oven was increased to 30 °C. After 35 minutes of heating at 30 °C (Nursultanov et al. 2017), each block was energised and the electrical data was recorded. These steps were repeated up to 90 °C, with a temperature step of 10 °C. Afterwards, each plastic enclosure with the block was weighed, to determine moisture loss. Finally, after removal from the plastic enclosure, each block's green volume was measured using the water displacement method, and then the block was left inside the oven at 105 °C until it reached a constant oven-dry mass.

Knowing the blocks' dimensions and the voltage and current, the EC was calculated as:

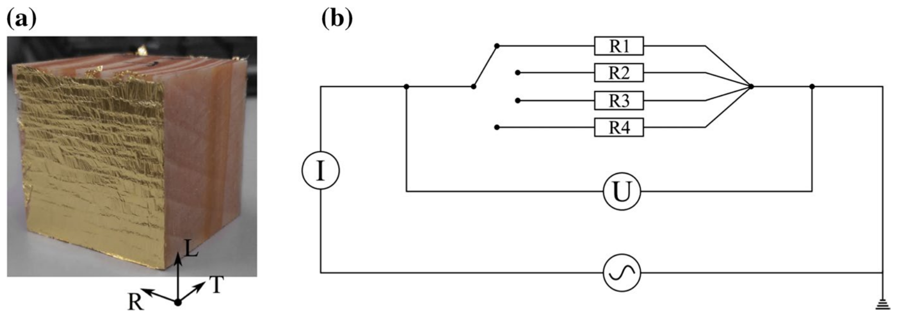

Fig. 2 **a** Block of *P. radiata*, with the contact surfaces covered with golden leaves, and **b** schematic diagram of the experimental set-up

$$\sigma = \frac{l \cdot I}{U \cdot A}, \tag{3}$$

where σ is the EC [$\mathrm{S\,m^{-}1}$]; l is the length of the block, along which the electrical current flows (m); I is the electrical current (A); U is the voltage across the block (V); and A is the cross-sectional area of the contact surface (m^2). In the four blocks with various extents of dryness, the electrical current flow would have largely avoided the dry patches. However, it was assumed that the electrical current flowed uniformly through the whole cross-sectional area to calculate the blocks' equivalent electrical conductivities using Eq. (3). The moisture content and basic density were determined as:

$$MC = \frac{m_g - m_o}{m_o} \cdot 100\%, \tag{4}$$

$$BD = \frac{m_o}{V_g}, \tag{5}$$

where X is the moisture content (%), m_g is the green mass (Kg), BD is the basic density ($\mathrm{Kg\,m^3}$), V_g is the green volume (m^3), and m_o is oven-dry mass (Kg) (Tables 1 and 2).

Results

Green samples

Variation of EC with temperature

All samples showed a positive monotonic correlation between EC and temperature. Within the selected temperature range, the average EC across all wood zones and grain directions increased by between 150% for *E. globoidea* and about 600% for *P. menziesii* and *P. radiata* from Ashley forest (Fig. 3). In *P. menziesii* and *S. sempervirens*, the average increase in the tangential EC was slightly higher than that of the radial EC, and about twice that of the longitudinal EC. In *P. radiata* from Ashley and Owen River forests, the average increase in the tangential EC was approximately twice that of the radial EC and three-times that of the longitudinal EC. On average the longitudinal EC of softwood sapwood increased by 240%. Conductivity of *E. globoidea* was enhanced on average by a factor of 3 in all directions for SW and HW. Overall, the increase in the longitudinal EC in the softwood species and EC of *E. globoidea* (in all directions and at all wood zones) was near linear, following the increase in the reciprocal of water viscosity.

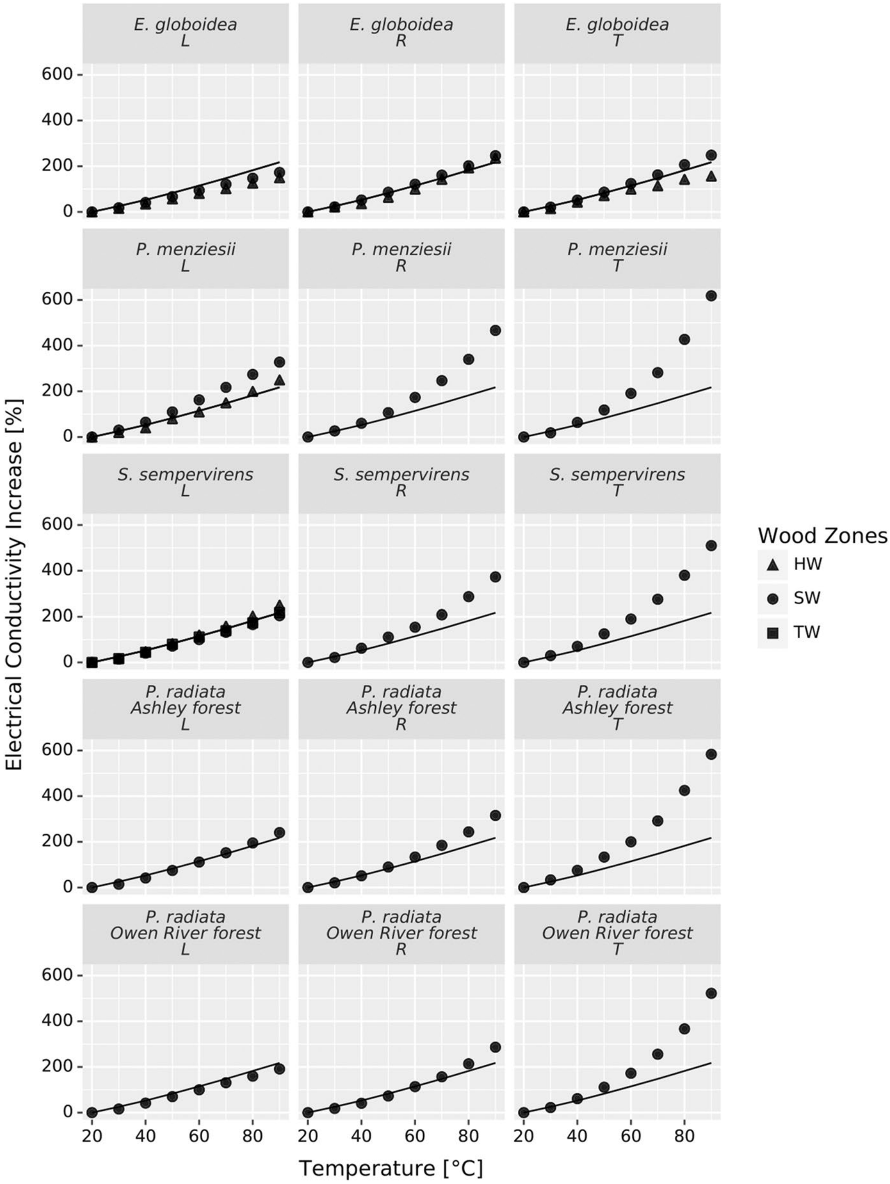

Fig. 3 Average increase in EC across all wood zones and grain directions from 20 to 90 °C. The solid black line denotes the reciprocal water viscosity (White 2011)

Relative values of EC

EC varied between wood zones, where the most and least conductive zones were SW and HW, respectively. In *S. sempervirens* (Fig. 4) and *E. globoidea* (Fig. 5), the ratios between the SW and HW longitudinal conductivity were two and four,

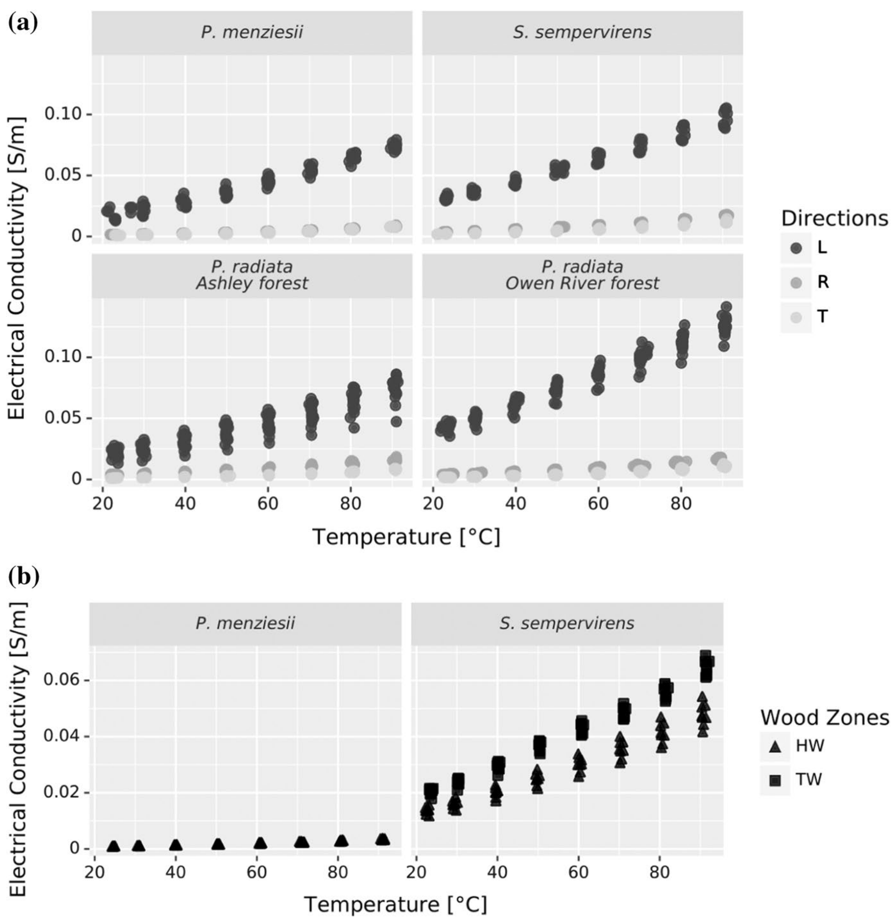

Fig. 4 Effect of temperature on **a** the sapwood EC and **b** the other wood zones' longitudinal ECs of the studied softwood species

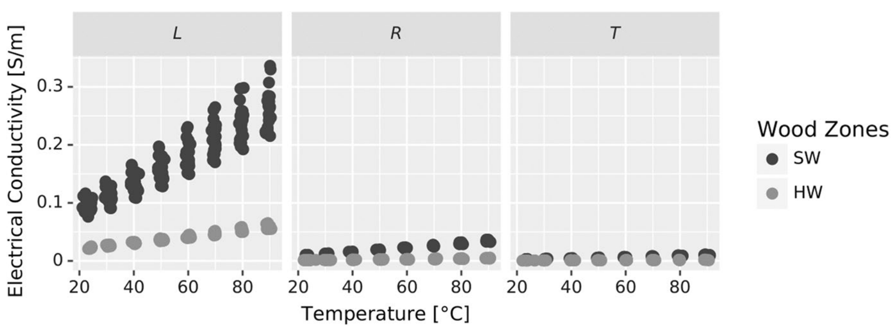

Fig. 5 Effect of temperature on the EC of *E. globoidea* in the L, R, and T directions

respectively; these values remained relatively constant over the whole temperature range. The transitional wood of *S. sempervirens*, with 145% MC, was slightly more conductive than the HW, with 183% MC (Fig. 4b). A negative MC to EC correlation was also observed in *E. globoidea*, where the SW and HW moisture contents were 161% and 174%, respectively. The most pronounced difference between heartwood and sapwood ECs was in *P. menziesii* (Fig. 4), where the ratio of SW (161% MC) to HW (49% MC) was approximately 17 at 20 °C, increasing to 20 at 90 °C. Sapwood EC of *E. globoidea* was seven-times higher than heartwood EC in the R direction and about five-times higher in the T direction (Fig. 5); these ratios were relatively temperature independent.

Table 3 shows sapwood EC normalised based on the conductivity of *E. globoidea*. At 20°C, SW of *E. globoidea* was twice as conductive as SW of *P. radiata* from Owen River forest in the L and R directions. This difference was approximately the same at 90°C. In the T direction, *E. globoidea* had the most conductive sapwood at 20°C; however, at 90°C, the most conductive SW was in *S. sempervirens*.

All wood species were the most conductive in the longitudinal direction, while radial EC was slightly greater than tangential conductivity. The average radial and tangential ECs of *E. globoidea's* sapwood were 9 and 33 times lower than the longitudinal EC at 20 °C, respectively (Fig. 6). These ratios changed with temperature to the respective values of 7 and 26 at 90 °C, indicating a higher temperature coefficient of EC in the R and T directions than that in the longitudinal direction. In *E. globoidea's* heartwood, the L/R and L/T conductivity ratios were 16 and 33, respectively, at 20 °C; the values decreased slightly to 12 and 32, at 90 °C. In the softwood species, these ratios were lower and varied within a range of 6–12 for the L/R and 16–24 for the L/T, at 20 °C. These ratios decreased by a factor of 1.5 and 2 for the L/R and L/T, respectively, at 90 °C. The most conductive in the L direction among tested softwood species was *P. radiata* from Owen River forest. It was about twice as conductive as *P. radiata* from Ashley forest in the L direction, but comparable in the other directions. This relation remained unchanged over the whole temperature range. At 20 and 90 °C, the longitudinal ECs of *P. radiata* from Owen River forest were 0.043 and 0.126 S m⁻1, respectively.

Table 3 Sapwood EC normalised based on EC of *E. globoidea* in the L, R, and T directions

Species	Directions		
	L (20 °(C)/90°(C))	R (20 °C/90°C)	T (20 °C/90°C)
E. globoidea	1.00/1.00	1.00/1.00	1.00/1.00
S. sempervirens	0.34/0.38	0.37/0.51	0.69/1.21
P. menziesii	0.18/0.29	0.15/0.25	0.38/0.78
P. radiata (Ashley forest)	0.23/0.29	0.39/0.47	0.41/0.81
P. radiata (Owen River forest)	0.46/0.49	0.44/0.49	0.62/1.11

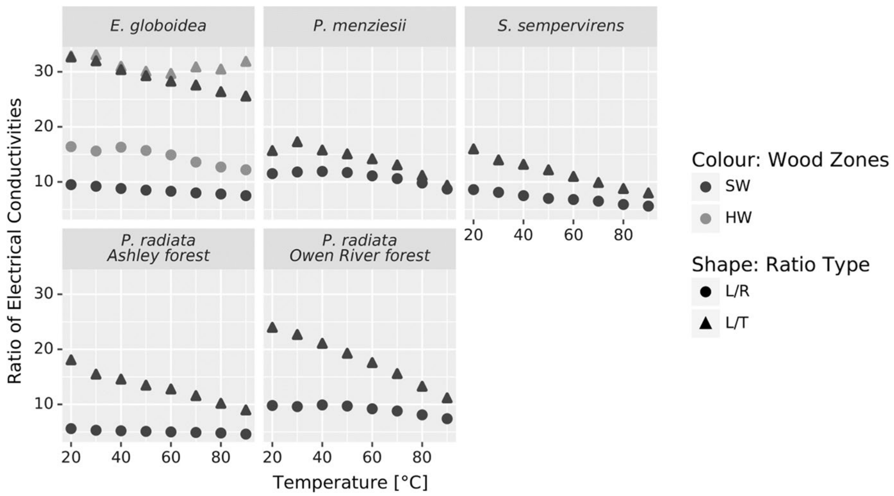

Fig. 6 Ratios of the longitudinal EC to the radial and tangential ECs, as a function of temperature

Effect of partial dryness

EC of the four selected additional, partially dry *P. radiata* sapwood blocks from Owen River forest was measured from 20 to 90 °C (Fig. 7). The EC of Block 1, with 195% MC, was similar to the EC observed in fully wet *P. radiata* blocks. However, at about room temperature, the conductivity of Block 9, with 30% MC, was 0.001 S m^{-}1. This is similar to the EC of the heartwood of *P. menziesii*. The effective conductivities of Blocks 4 and 7 were comparable and were higher than that of Block 9, but significantly lower than that of Block 1.

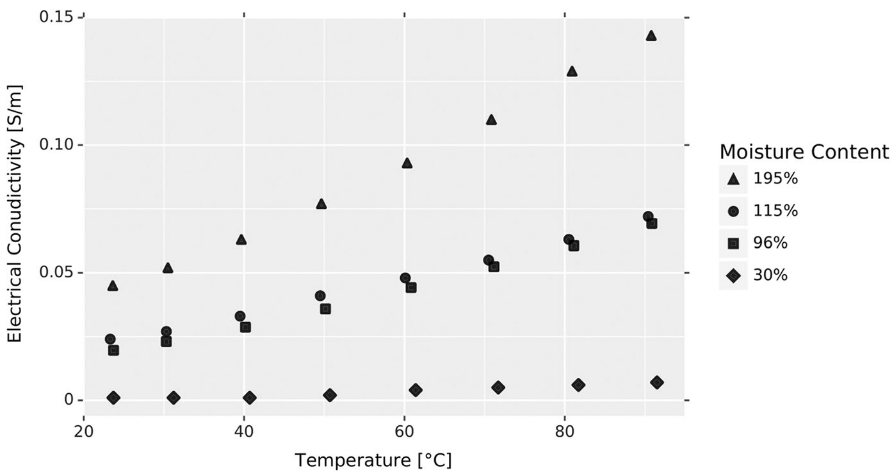

Fig. 7 Effect of temperature on EC of *P. radiata* blocks, with dry patches, in the longitudinal direction

Discussion

In all studied species, the L conductivity increased by a factor of three and followed the increase in reciprocal of water viscosity reasonably closely (Fig. 3). Such behaviour indicates that an electrical current flows predominantly through wood openings in the L direction due to continuous water columns formed by longitudinally aligned wood tissue (tracheids for softwood and vessels for hardwood) (Butterfield 2006). In the R and T directions of the softwood species, the EC increase followed the reciprocal of water viscosity below 50 °C, suggesting that an electrical current flows through wood openings: radial rays and pits. However, above 50 °C, the EC increased faster than the reciprocal of water viscosity, indicating that some additional paths became available for the current conduction. Since, the number of wood openings within wood structure is conserved, the EC rise was presumably caused by establishment of current paths through cell walls starting from 50 °C. This hypothesis is well-supported by diffusion through the cell wall, as it increases exponentially with temperature (Langrish and Walker 2006; Stamm 1964). In *E. globoidea*, however, the R and T conductivities increased at the same rate as the reciprocal of water viscosity, indicating that current conduction through openings dominates diffusion, over the tested temperature range.

All wood samples showed anisotropic behaviour, with the longitudinal and tangential ECs being the highest and lowest, respectively (Fig. 4 and 5). Similar behaviour was observed by Stamm (1927) and Nursultanov et al. (2017), and is linked to the longitudinal alignment of wood tissue. In the R direction, there are radial rays that form continuous current conduction paths, making the R conductivity higher than the T conductivity (Nursultanov et al. 2017). EC of *E. globoidea* in the L and R directions was at least twice as high as that of the other species (Table 3), potentially due to the larger size of *E. globoidea* vessels and radial rays, along with perforation plates. The mean tangential diameter of *E. globoidea* vessels is 175 mm (Dadswell 1972), while PR tracheids' mean tangential diameter is 40 mm (Harris 1991). *E. globoidea* and PR have approximately 10 and 6 rays per millimetre in tangential longitudinal section, respectively (Dadswell 1972; Harris 1991). Unlike softwood pits, perforation plates do not have separating membranes (Butterfield 2006), resulting in wider wood openings. Thus, the wider lumen diameter and the greater the number of rays and perforation plates, the easier the movement of ions and the higher the conductivity. The tangential EC of *E. globoidea* was comparable with that of the softwood species (Table 3), indicating that hardwood species conduct electrical current similarly to softwood species in the T direction, through pits and cell walls. In addition, the R and T conductivities at 20°C showed good agreement with the data obtained by Guyot et al. (2013) and Luo (2019) using ERT, indicating that the ERT method estimates predominantly transverse (a combination of R and T) resistivity distribution.

Sapwood was more conductive than heartwood in all studied species. In *P. menziesii*, such behaviour can be linked to the MC difference between SW and HW, 143% and 49%, respectively. According to Stamm (1964), conductivity can drop by a factor of 50 from complete saturation to FSP. However, the *S. sempervirens* and *E. globoidea* samples show that, significantly above FSP, MC cannot explain EC differences between wood zones. For example, in *S. sempervirens*, the average MC of HW and TW were 183% and 145%, respectively, but the TW conductivity of 0.02 S m^-1 was higher than that of HW (0.014 S m^-1). There thus appear to be additional factors that can affect EC differences between HW and SW near complete saturation, such as ionic composition (Skaar 1988), permeability (Stamm 1970, 1972), and availability of living cells (Butterfield 2006). Stamm (1964) reported that ECs of heartwood and sapwood in *P. elliottii* are comparable, being around 0.015 S m^-1 at near room temperature and 180% MC. Studying *Q. robur* by means of the ERT method, Bieker and Rust (2010) found that the inner heartwood was more conductive than the outer heartwood. However, all these studies, including this research, are based on a small sample size, and hence further research is required to isolate the mechanism of current conduction in HW and SW.

The longitudinal HW conductivity of *S. sempervirens* showed good agreement with that measured by Stamm (1929), 0.019 S m^-1 at room temperature and 150%. The SW conductivity, however, was twice that measured by Stamm (1929). The difference between the results was assumed to be due to ionic content variation within the sap, which in turn can depend on ionic concentration in soil (Munns 1988). This hypothesis is supported by EC differences between *P. radiata* from Ashley forest and Owen River forest, where the latter is about twice as conductive as the former and similar to that reported by Nursultanov et al. (2017). Future testing, with a larger sample size, is required to investigate the dependence of EC on ionic content of soil. Finally, the effect of dryness on EC of PR showed that dry patches decrease the conducting surface area, causing the increase in overall resistance. Hence, the partially dry cubes behaved as a combination of fully saturated wood, in the wet patches, and near FSP wood, in the dry patches, with the current flowing predominantly through the wetter regions.

Conclusion

This research agreed with earlier findings by Nursultanov et al. (2017), showing that EC of green wood is highly dependent on temperature and grain orientation. The EC temperature dependence varies between wood species and trees, with the most distinguishable difference occurred between hardwood and softwood species. It was hypothesised that electrical current conduction in hardwood is unconstrained by the wood structure, due to wider wood openings. In softwood species, however, electrical current has to flow through narrower wood openings and, above 50 °C, through new conduction paths within cell walls. In addition, it was hypothesised that EC variation between trees and wood zones can be due to ionic content variation within sap. To test these hypothesis, future testing with a larger sample size is required.

Acknowledgements The authors are thankful to Mr. Graham Mitchell for his help in building the testing rig. The authors also wish to thank Rayonier Matariki Forests and New Zealand Dryland Forests

Initiative, with Mr Paul Millen, for providing freshly sawn logs used in this research. This work has been supported by Scion under the NZ Ministry of Business, Innovation and Employment (MBIE) and Stakeholders in Methyl Bromide Reduction (STIMBR) funded Market Access Programme, and Specialty Wood Products Research Partnership.

References

Bard AJ, Faulkner LR (2001) Electrochemical methods: fundamentals and applications, 2nd edn. Wiley, New York

Berry SL, Roderick ML (2005) Plant-water relations and the fibre saturation point. New Phytologist 168(1):25–37

Bieker D, Rust S (2010) Electric resistivity tomography shows radial variation of electrolytes in quercus robur. Canad J Forest Res 40(6):1189–1193

Butterfield B (2006) The structure of wood: form and function. In: Walker JCF (ed) Primary wood processing. Springer, The Netherlands, pp 1–22

Dadswell HE (1972) The anatomy of eucalypt woods. CSIRO Melbourne, Canberra

Fleischer HO, Downs LE (1953) Heating veneer logs electrically. Tech. rep, United States Department of Agriculture, Forest Service, Forest Products Laboratory

Glass SV, Zelinka SL (2010) Moisture relations and physical properties of wood. In: Wood handbook-wood as an engineering material. General Technical Report FPL-GTR-190, Department of Agriculture, Forest Service, Forest Products Laboratory, Madison, WI: US, pp 4.1–4.19

Guyot A, Ostergaard KT, Lenkopane M, Fan J, Lockington DA (2013) Using electrical resistivity tomography to differentiate sapwood from heartwood: application to conifers. Tree Physiol 33(2):187–194

Harris JM (1991) Structure of wood and bark. In: Kininmonth JA, Whitehouse LJ (eds) Properties and uses of New Zealand radiata pine. Ministry of Forestry, Forest Research Institute with assistance from the New Zealand Lottery Grants Board, Rotorua, New Zealand, pp 21–216

Haynes WM (2014) CRC handbook of chemistry and physics. CRC Press, Boca Raton

Heffernan W, Nursultanov N, van Herel R, Smart T (2018) Joule heating of logs for phytosanitary purposes and timber processing pre-treatment. Adv Mater Lett 9(11):767–775. https://doi.org/10.5185/amlett.2018.2133

Hoover K, Uzunovic A, Gething B, Dale A, Leung K, Ostiguy N, Janowiak JJ (2010) Lethal temperature for pinewood nematode, bursaphelenchus xylophilus, in infested wood using microwave energy. J Nematol 42(2):101

Khaled AY, Aziz SA, Bejo SK, Nawi NM, Seman IA, Onwude DI (2018) Early detection of diseases in plant tissue using spectroscopy applications and limitations. Appl Spectrosc Rev 53(1):36–64. https://doi.org/10.1080/05704928.2017.1352510

Kuroda N, Tsutsumi J (1982) Anisotropic behaviour of electrical conduction in wood. Mokuzai Gakkaishi 28:25–30

Langrish T, Walker JCF (2006) Drying of timber. In: Walker JCF (ed) Primary wood processing. Springer, Dordrecht, pp 251–295

Luo Z, Guan H, Zhang X (2019) The temperature effect and correction models for using electrical resistivity to estimate wood moisture variations. J Hydrol 578:124022

McCleskey RB (2011) Electrical conductivity of electrolytes found in natural waters from (5 to 90) ° C. J Chem Eng Data 56(2):317–327

Munns R (1988) Effect of high external NaCl concentrations on ion transport within the shoot of Lupinus albus. I Ions Xylem Sap Plant Cell Environ 11(4):283–289

Nursultanov N (2018) Joule heating of green *Pinus radiata* logs for phytosanitary purposes: an in-depth investigation by experimentation and computational modelling. PhD thesis, Chemical and Process Engineering Department, College of Engineering, University of Canterbury, New Zealand

Nursultanov N, Altaner C, Heffernan WJB (2017) Effect of temperature on electrical conductivity of green sapwood of Pinus radiata (radiata pine). Wood Sci Technol 51(4):795–809. https://doi.org/10.1007/s00226-017-0917-6

Nursultanov N, Heffernan WJB, van Herel MJWMR, Nijdam JJ (2019) Computational calculation of temperature and electrical resistance to control joule heating of green Pinus radiata logs. Appl Therm Eng 159:113855. https://doi.org/10.1016/j.applthermaleng.2019.113855

Oletic D, Bilas V (2020) How thirsty the crops are: emerging instrumentation for plant-based field measurement of water stress. IEEE Instrum Measure Magz 23(2):37–46
Skaar C (1988) Wood-water relations. Springer, Berlin
Stamm AJ (1927) The electrical resistance of wood as a measure of its moisture content. Ind Eng Chem 19(9):1021–1025
Stamm AJ (1929) The fiber-saturation point of wood as obtained from electrical conductivity measurements. Ind Eng Chem Anal Edition 1(2):94–97
Stamm AJ (1930) An electrical conductivity method for determining the moisture content of wood. Ind Eng Chem Anal Edn 2(3):240–244
Stamm AJ (1960) Bound-water diffusion into wood in across-the-fibre directions. Forest Products J 10(10):524–8
Stamm AJ (1964) Wood and cellulose science. Ronald Press Co., New York
Stamm AJ (1970) Maximum effective pit pore radii of the heartwood and sapwood of six softwoods as affected by drying and resoaking. J Soc Wood Sci Technol 1(4):263–269
Stamm AJ (1972) Maximum effective vessel diameters of hardwoods. Wood Sci Technol 6(4):263–271
White FM (2011) Fluid mechanics, 7th edn. McGraw-Hill, Singapore
Zelinka SL, Glass SV, Stone DS (2008) A percolation model for electrical conduction in wood with implications for wood-water relations. Wood Fiber Sci 40(4):544–552
Zelinka SL, Gleber SC, Vogt S, López GMR, Jakes JE (2015) Threshold for ion movements in wood cell walls below fiber saturation observed by x-ray fluorescence microscopy (XFM). Holzforschung 69(4):441–448

Publisher's Note Springer Nature remains neutral with regard to jurisdictional claims in published maps and institutional affiliations.